

EFFICIENT IMPLEMENTATION OF A COMPONENT-BASED JOINT MODEL

A. ALHASAWI^{*}, S. GUEZOULI AND M. HJIAJ

^{*} National Institute of Applied Sciences (INSA de Rennes)
Université Européenne de Bretagne
20, avenue des Buttes de Coësmes –CS 70839- 35708 Rennes cedex 7 France
anas.alhasawi@insa-rennes.fr
samy.guezouli@insa-rennes.fr
mohammed.hjiaj@insa-rennes.fr

Key words: Steel joint connection, Cyclic load, Components-based model, Moment-rotation curve.

Abstract. This paper deals with a nonlinear analysis of beam-to-column steel joint. The connection uses an end-plate welded to the steel cross-section of a steel-concrete composite beam and bolted to the column flange. The proposed model developed herein combines the knowledge of prior studies that used the component-based approach, on one hand and the Finite Element algorithms in plasticity, on second hand. The originality of this work is to efficiently take into account possible gaps between the end-plate and the column flange in case of plastic deformation of some components of the joint during the cyclic loading. The numerical investigation aims to predict the behavior of this type of joint in presence of the gap during the cyclic loading.

1 INTRODUCTION

End-plate connection is very popular for steel frames because of its simplicity and its economy in fabrication and construction. Usually, there are two assumptions in the design of such type of joint: a pinned joint or a fully rigid joint. However, it is widely known that both assumptions are very far from the real joint behavior and the assumption of a semi rigid joint appears more realistic and also economic [1].

Nowadays, many research studies on the behavior of semi-rigid joints under monotonic loading. These studies focused on the evaluation of the moment resistant, the rotational stiffness and the rotational capacity (ductility) [2-7]. However, there are fewer efforts to study the joint behavior under cyclic loading.

For the first time, the proposed model of joint developed herein takes into account the plastic deformation of one or more components within the joint and includes possible presence of a gap between the end-plate and the column flange during the cyclic loading history. It worth to remind that Eurocode 3 [8, 9] refers to this phenomenon threw the collapse models of the T-stub test (Figure 1) leading to three failure models that could occur because of the thread stripping on the bolts.

This work addresses the cyclic nonlinear analysis of bolted steel joints in building frames. The aim in this work is to develop a mechanical model for this type of joint taking benefit from the knowledge of prior studies that used the component-based analysis on one hand, and

taking into account some realistic phenomena that have never been considered before, on second hand.

The proposed joint model has been tested for the gap problem in a simple case of extended end-plate with two bolt-rows (one at the top and the other at the bottom of the joint – Figure 2).

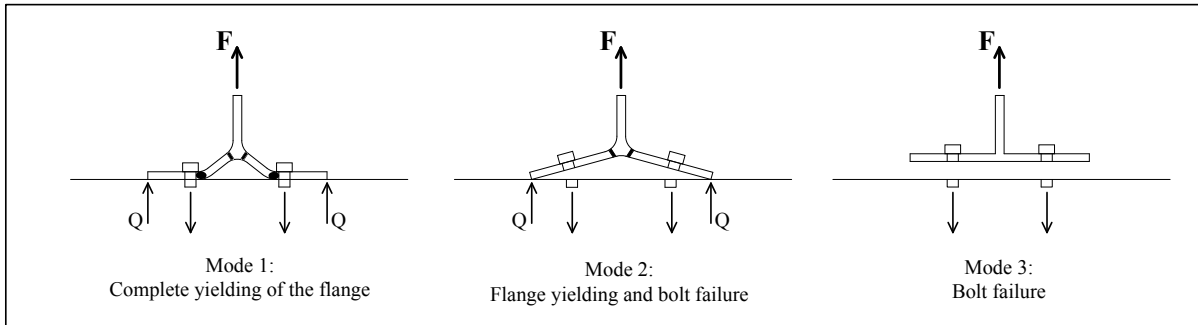


Figure 1: Failure Modes - T-Stub test

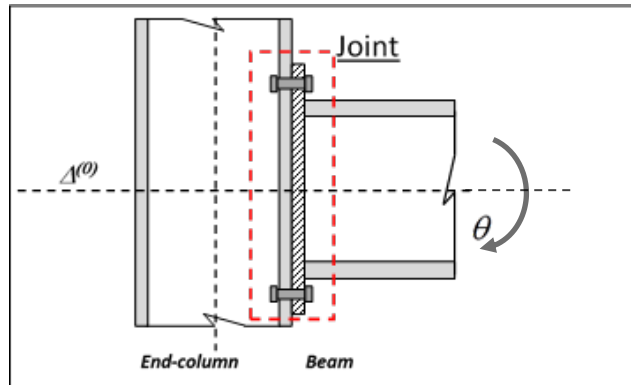


Figure 2: Example to test the gap problem

2 COMPONENT-BASED ANALYSIS

The component-based analysis has been clearly described in Eurocode 3 (Annex J). Each part of the joint (Table 1) represents a component that is replaced by a uniaxial spring with its own behavior. It worth to remind the active resistance of each component in order to understand the global behavior of the joint. The beam web and flange in compression can be grouped in one effect noted: BWFC. The column web panel in shear has not been considered herein because this model concerns only the joint as defined in Figure 2.

Table 1: List and effect of different components

Component	Effect
Steel Beam	
BWT	Beam Web Tension
BWC	Beam Web Compression
BFC	Beam Flange Compression

BFT	Beam Flange Tension
Bolt	
BT	Bolt Tension
End-Plate	
EPB	End Plate Bending
Steel Column	
CFB	Column Flange Bending
CWT	Column Web Tension
CWC	Column Web Compression

The principle of the component-based analysis is to combine the active components located at a same level to get an equivalent component and therefore to combine all equivalent components to get the stiffness matrix of the joint.

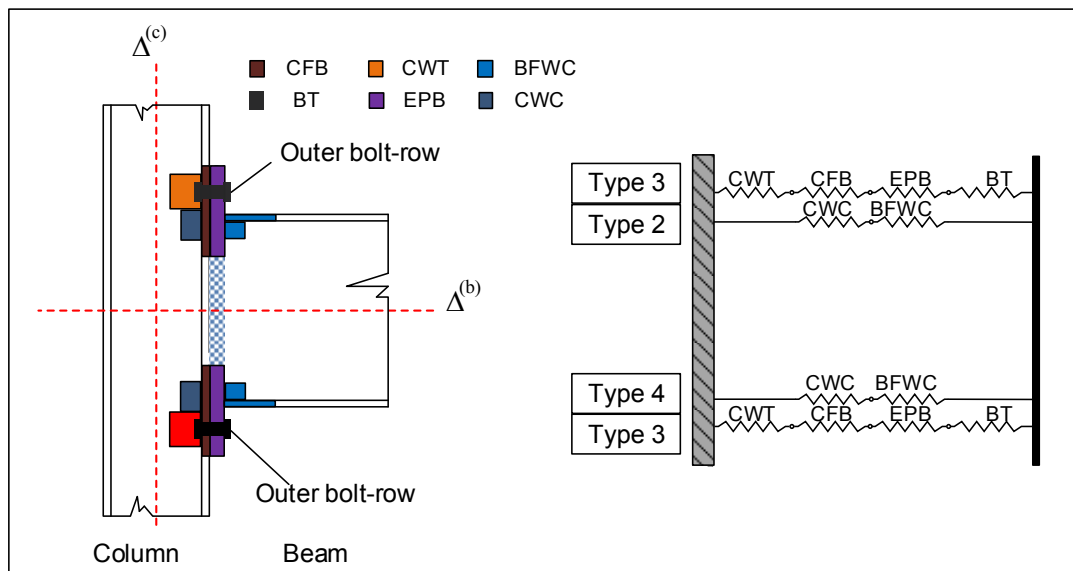


Figure 3: Components effects and equivalent component Types

Each component remains in the elastic range and defines its elastic stiffness so-called initial stiffness and noted: k_{ini} . In the scope of this work, the behavior of each component is extended to the elastic-plastic range with or without material hardening (Figure 3).

- The Types 2 and 4 include the beam flanges and resist only in compression. They contain the same components but the Type 2 located at the top beam flange level and the Type 4 at the bottom one. During the cyclic loading (rotation θ), they are activated alternatively. Only in case of pure compression of the whole joint, they can be activated together.
- The Type 3 includes the bolts and resists only in tension. The number of equivalent components of Types 3 depends on the number of the bolt-rows. During the cyclic loading only the bolt-rows being in tension are activated.

3 STIFFNESS MATRIX OF THE JOINT

The proposed model is based on the component method, it consists of two rigid links which represent the column centerline on the right side and the end-beam line on the left side (Figure 4). Both lines are connected by series of springs that represent the joint equivalent components. In case of more than two bolt-rows (Type 3), one uses following notation:
 - $T2$ and $T4$ for Type 2 and Type 4 respectively,
 - $T3$ for Type 3 followed by: t_i ($i = 1, \dots, n$) or b_i ($i = 1, \dots, m$); n and m represent respectively the number of bolt-rows above (t_i) and below (b_i) the reference axis (load axis).

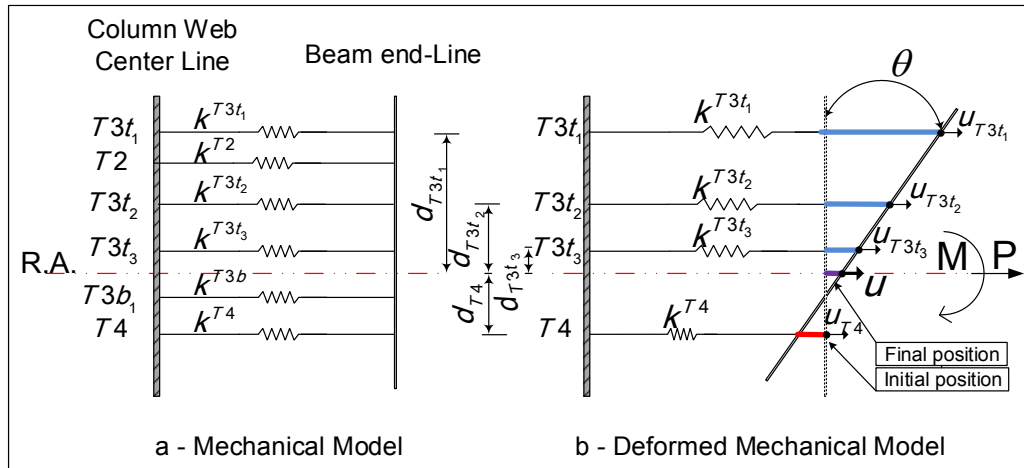


Figure 4: Proposed mechanical model for the joint

Figure 4, gives the details of the proposed mechanical model and shows a deformed state in case of negative bending. Only $T3t_i$ and $T4$ (bottom beam-flange) have been activated and other equivalent components have been disabled. At each equivalent component level, corresponding stiffness k and lengthening (shortening) u are highlighted while at the reference axis (R.A.) the global variables of the joint appear as a couple (u, θ) representing respectively the axial displacement and the rotation of the joint. This variables are related to the applied loads (P, M) representing the axial force and the negative bending moment, respectively. It is clear that in case of positive bending, equivalent components of types $T3b_i$ and $T2$ (top beam-flange) will be activated and precedent ones will be disabled.

The global force vector can be defined as follows:

$$F = \{P \quad M\}^T \tag{1}$$

and corresponding global displacement vector is:

$$U = \{u \quad \theta\}^T \tag{2}$$

The displacement of each equivalent component can be geometrically calculated in case of small rotations, as follows:

$$\begin{aligned} u_{T3i} &= u + d_{T3i} \sin \theta \Leftrightarrow u_{T3i} = \{1 \quad d_{T3i}\} U \\ u_{T2} &= u - d_{T2} \sin \theta \Leftrightarrow u_{T2} = \{1 \quad -d_{T2}\} U \end{aligned} \quad (3)$$

By summing the stiffnesses corresponding to all the equivalent components, the stiffness matrix of the joint can be written as follows:

$$K = \begin{bmatrix} k^{T2} + \sum k^{T3i} & \sum d_{T3i} k^{T3i} - d_{T2} k^{T2} \\ \sum d_{T3i} k^{T3i} - d_{T2} k^{T2} & \sum d_{T3i}^2 k^{T3i} + d_{T2}^2 k^{T2} \end{bmatrix} \quad (4)$$

And finally, the equations to solve are:

$$F = KU \quad (5)$$

A displacement control procedure is adopted to load the specimen and the arc-length method to solve the non-linear system of equations (mechanical non-linearity) (Eq. 5).

4 SOLUTION FOR THE PROBLEM OF THE GAP

4.1 The T-Stub

Equivalent component of Type 3 is active only in tension; during a cyclic loading it could happen that one of its components reaches the plastic range. The concerned components are those whom resist in tension (CWT, CFB, EPB, BWT, BT) A well-understanding of the mechanism of such equivalent component type implies to present the T-Stub model and its three failure modes (Figure 1 – [10]).

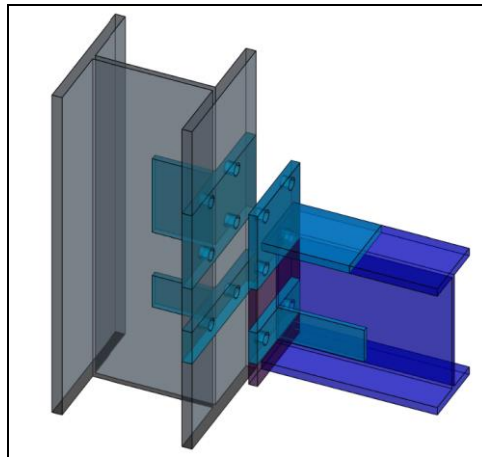


Figure 5: Different T-Stub orientations

The possible collapse mechanism of the T-Stub connection with one bolt row are:

- A complete yielding of the flange for the first mode leads to four plastic hinges, two are located at the bolt axes and the others at the flange to web connection,
- There are two plastic hinges for the second mode located at the flange to web connection,

- No plastic hinges for the third one because the collapse due to the bolts failure only.

Figure 5 shows the location of different T-Stub orientations (horizontal and vertical) included within an end-plate bolted connection:

- The first T-Stub appears horizontal and represents the tension located between the beam flanges. For this T-Stub, the equivalent component of Type 3 includes 5 components (CWT, CFB, EPB, BWT, BT)
- The second T-stub appears vertical and represents the tension zone of the extended end-plate. For this T-Stub, the equivalent component of Type 3 includes only 4 components (CWT, CFB, EPB, BT).

4.2 Deformation analysis of the specimen

The equivalent component of Type 3 requires special attention and one distinguishes two states:

- First state: Compression state. This case is easy to solve because Type 3 does not resist in compression.
- Second state: Unloading state. This state requires the development of different stages of loading-unloading cycles.

One notes:

ΔN_m : the increment of axial force located at the equivalent component level “m” of Type 3 between two successive loading steps ($I+1$) and (I): $\Delta N_m = N_m^{(I)} - N_m^{(I-1)}$.

- *First Loading-Unloading of the joint (the top bolt-row is active $\Delta N_m^{top} \geq 0$)*

Supposing that the first Loading-Unloading of the joint begins by a negative bending therefore, the gap at the top beam flange level appears. In this case, the T-stub model is represented by the top beam-flange. After the unloading, plastic deformations remain in some components of Type 3 that generates the so-called gap.

Figure 6 shows the first loading-unloading stage with corresponding force displacement curve of the Type 3 and moment-rotation curve for the joint.

If the unloading occurs while the bolt remain in the elastic range, the gap is recovered in case of total unloading (the column flange and the end-plate remain in full contact with the bolt).

- *Second Loading-Unloading of the joint (the bottom bolt-row is active $\Delta N_m^{bottom} \geq 0$)*

The second half of a total loading cycle begins by reloading the specimen with a positive bending. In order to close the precedent gap, a slip must occur in the curve ($F_t - u_t$).

This slip that allows the bottom bolt-row to be activated, is equal to the precedent gap and corresponds to the cumulative permanent displacements occurred during the precedent Loading-Unloading stage. Consequently, the effect on the joint curve ($M - \theta$) appears clearly in. After the unloading of this second stage, another gap appears in the bottom beam-flange level.

At this stage, two gaps that should be closed before beginning the second loading cycle. During closing the gap, there is a slip in the moment rotation curve as presented in Figure 7.

Following Loading-Unloading cycles use the same procedure taking care to close the gaps before each beginning of reloading.

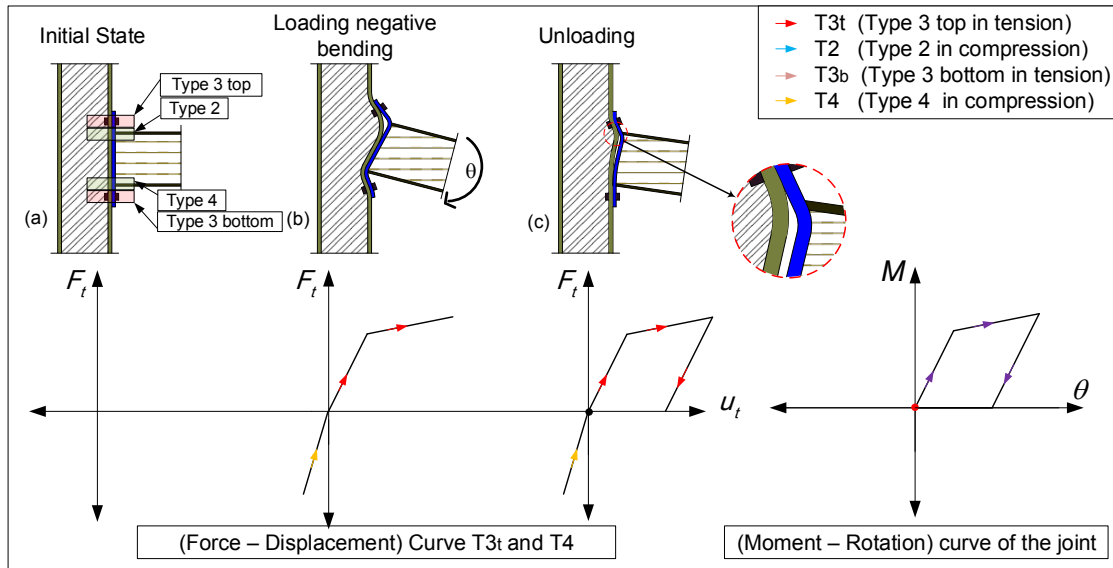


Figure 6: First Loading-Unloading stage (half cycle)

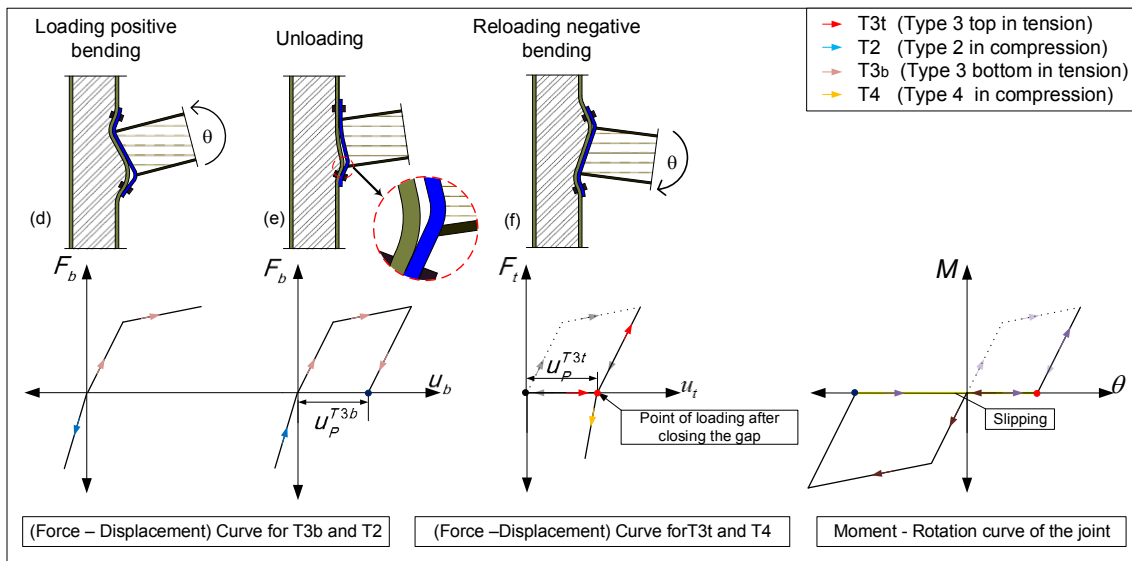


Figure 7 Second Loading-Unloading stage (complete cycle) - Beginning of second cycle

5 VALIDATION OF THE SOLUTION PROPOSED FOR THE GAP

The solution proposed for the gap is validated using the example presented in Figure 2 with the geometrical characteristics presented in Figure 8. Only a rotation θ is applied to the joint in accordance with the cyclic loading history presented in Figure 9. The corresponding mechanical model is given in Figure 10 and material properties of the proposed example are obtained from [1] and summarized in Table 2 and Initial stiffness k^{ini} as-well-as elastic

resistance F^{el} are given in Table 3. It worth to point out that the elastic resistance considered for an equivalent component is the minimum of the ones of each included component; the restrained values are highlighted in Table 3.

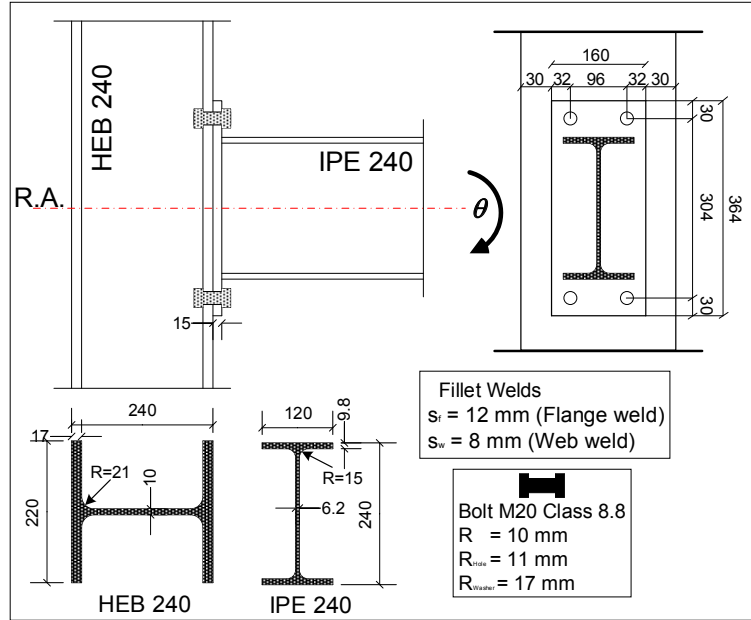


Figure 8: Geometrical characteristics

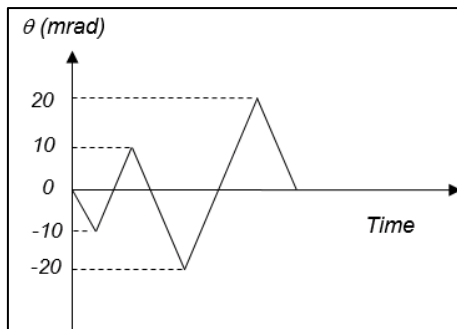


Figure 9: Cyclic loading history

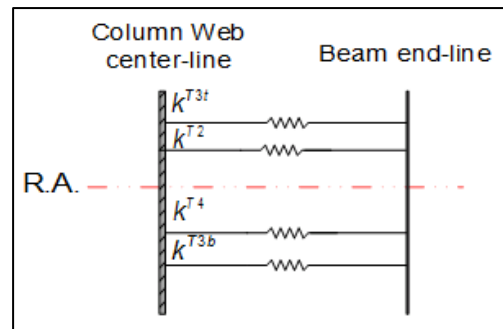


Figure 10: Mechanical model

Table 2: Material properties (MPa)

Material	Component	Tensile strength (f_y)	Young's Modulus
Steel S275	BW	363.40	203713
Steel S275	BF	340.14	215222
Steel S275	CW	372.02	206936
Steel S275	CF	342.95	220792
Steel S275	EP	369.44	200248

M20	Bolts		900	200000		
Table 3: Initial stiffness and resistance force (kN/mm and kN)						
Component	T3t and T3b		T2		T4	
	k^{ini}	F^{el}	k^{ini}	F^{el}	k^{ini}	F^{el}
CFB	8499.7	311.3	-	-	-	-
EPB	4223.1	289.8	-	-	-	-
CWT	1476.3	533.2	-	-	-	-
BWT	-	-	-	-	-	-
BFWC	-	-	∞	541.6	∞	541.6
BWC	-	-	2133.6	656.7	2133.6	656.7
BT	1630.6	441.0	-	-	-	-

For each component within the joint, material hardening has been considered very light ($k^{ini}/100$) but not equal to zero. In accordance with the cyclic loading history (Figure 9), the (Moment - Rotation) curve obtained as the response of the joint behavior is given in Figure 10. It appears clearly that the gaps obtained at both top and bottom levels of the joint generate slipping at both sides of the zero-rotation axis of the curve (dashed arrows). Alternatively between top and bottom bolt-rows, the gap obtained by the tension of the top bolt-row for example, must be first recovered before beginning the tension at the bottom bolt-row. The proposed algorithm follows these sequences very rigorously in order to insure an accurate solution of the proposed model (the index t corresponds to the top bolt-row in tension and the index b to the bottom bolt-row in tension).

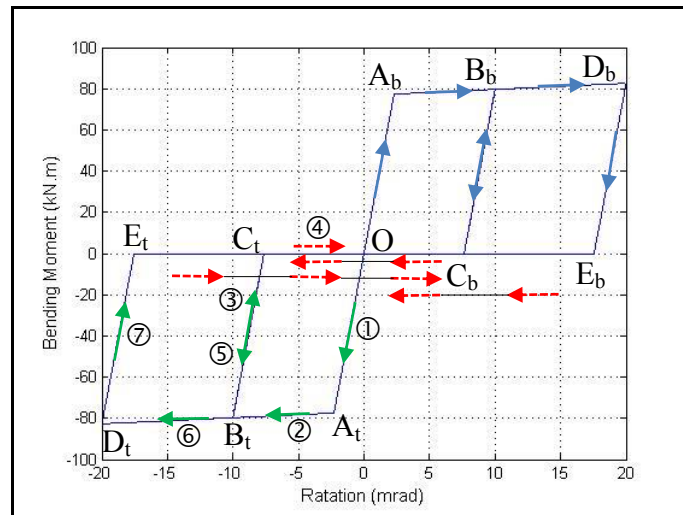


Figure 10: (Moment-Rotation) curve

First loading cycle (-10 mrad \leq θ \leq 10 mrad):

- (O – A_t – B_t) Loading in negative bending
- (B_t – C_t) Unloading T3t

$(C_t - O)$	Slipping
$(O - A_b - B_b)$	Loading in positive bending
$(B_b - C_b)$	Unloading $T3b$
$(C_b - O - C_t)$	Slipping

Second loading cycle $(-20 \text{ mrad} \leq \theta \leq 20 \text{ mrad})$:

$(C_t - B_t - D_t)$	Reloading in negative bending
$(D_t - E_t)$	Unloading $T3t$
$(E_t - C_t - O - C_b)$	Slipping
$(C_b - B_b - D_b)$	Reloading in positive bending
$(D_b - E_b)$	Unloading $T3b$

After each load cycle, the plastic deformation of the components within each equivalent component are cumulated. At the end of the unloading stage, permanent deformation defining the so-called gap needs to be closed before the beginning of the bottom bolt-row loading.

In accordance with Figure 11, following values of couples (Moment in kNm -Rotation in $mrad$) of the joints are obtained when the top bolt-row is active (same results when the bottom bolt-row is active because of symmetry):

First loading cycle $(-10 \text{ mrad} \leq \theta \leq 10 \text{ mrad})$:

$(O - A_t - B_t)$	$(0-0), (77.4-2.3), (79.7-10.0)$
$(B_t - C_t)$	$(79.7-10.0), (0-7.6)$
$(C_t - O)$	$(0-7.6), (0-0)$

Second loading cycle $(-20 \text{ mrad} \leq \theta \leq 20 \text{ mrad})$:

$(O - C_t)$	$(0-0), (0-7.6)$
$(C_t - B_t - D_t)$	$(0-7.6), (79.7-10.0), (82,6-20.0)$
$(D_t - E_t)$	$(82,6-20.0), (0-17.6)$
$(E_t - O)$	$(0-17.6), (0-0)$

The curves of Figure 12 are obtained by a video capture of the model in movement at the initial state and at the instant of maximum bending moment. Initial state (no loading) is also given in order to compare the spring lengths. It worth to precise that the couple of springs ($T3t - T4$) are active in same time and ($T3b - T2$) also, and both couples are active alternatively; therefore:

- Negative displacement obtained in the spring $T4$ (bottom beam-flange row) is due to a compression force while the tension is active in the spring $T3t$ (top bolt-row).
- Negative displacement obtained in the spring $T3b$ (bottom bolt-row) is due to a slipping (the spring does not support any compression force) while the positive displacement obtained in the spring $T2$ (top beam-flange row) is also a slipping (this row does not support any tension).

Figure 13 present the (force-displacement) curve of each row of the joint. The slipping values are obtained from these curves:

$$(C_t \rightarrow O) = 2.038\text{mm}$$

$$(E_t \rightarrow O) = 4.688\text{mm}$$

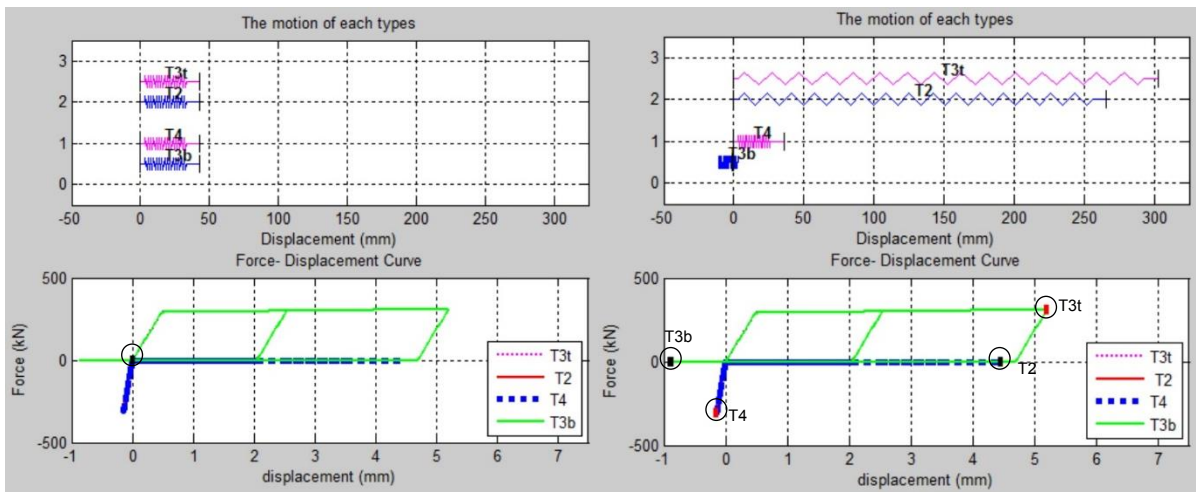


Figure 11: Springs motion during a cyclic loading – Initial and Maximum moment states

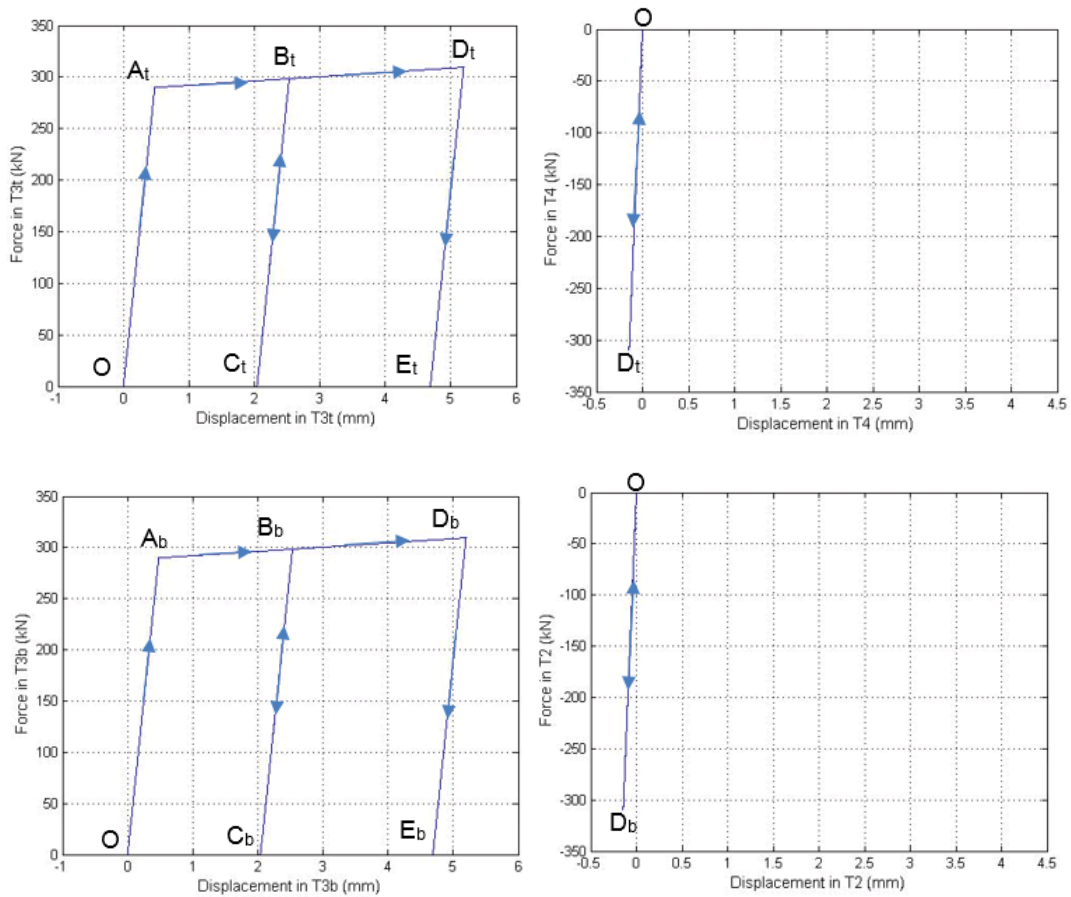


Figure 12: Force-displacement curves for each row of the joint

6 CONCLUSIONS

The performance of the beam-to-column joint model proposed in this paper is due to its simplicity. It appears as an easy-to-compute tool that is very useful in practice to be implemented in structural software to study frame behavior in dynamic for example. It is based on the component-based analysis that is nowadays well-known by the designers of the joints. It worth to precise that its performance has been extended to solve the problem of the gap that could appear between the column-flange and the end-plate during a cyclic loading. This problem has never been considered before, especially when it is included as a part of the plasticity algorithm. Special care during computation is required for several tests that have to be computed for the gap to control the plasticity of each component within the joint. This care insures to approach the real behaviour of the joint with appropriate slipping to recover the gaps. For further developments, the group effect of two or more bolt-rows have to be treated under monotonic loading and then under cyclic loading including the gap solution. At second time, the model could be extended to a composite beam connected to a steel column.

REFERENCES

- [1]. ALEXANDRE. ALMIDA. DEL. SAVIO, A COMPONENT METHOD MODEL FOR SEMI-RIGID STEEL JOINTS INCLUDING BENDING MOMENT-AXIAL FORCE INTERACTION, Rio de Janeiro: Civil Engineering Departement - PUC-Rio, 2008.
- [2]. B. M. Broderick, A.W. Thomson., "The response of flush end-plate joints under earthquake loading," *Journal of Constructional steel research*, no. 58, pp. 1161-1175, 2002.
- [3]. Eurocode 3 : Design of steel structure, Part 1.8: Design of Joints, European Committee for Standardisation (CEN).
- [4]. Frédéric. CERFONTAINE, Etude de l'interaction entre moment de flexion et effort normal dans l'assemblages de boulonnés, Liège: Université de Liège, 2004.
- [5]. Joshua Michael Taylor, NONLINEAR ANALYSIS OF STEEL FRAMES WITH PARTIALLY RESTRAINED COMPOSITE CONNECTIONS AND FULL OR PARTIALLY COMPOSITE GIRDERS, Georgia Institute of Technology, 1999.
- [6]. L. Simoes da Silva, Ana Girao Coelho "A ductility model for steel connections," *Journal of Constructional Steel Research*, no. 57, pp. 45-70, 2001.
- [7]. L. Simoes da Silva, Aldina Santiago, Paulo Vila Real "Post-Limit stiffness and ductility of end-plate beam-to-column steel joints," *Computers & Structures*, no. 80, pp. 515-531, 2002.
- [8]. P. C. da L.Nunes, L. R. O. da Silva, P. C. G. da S. Vellasco and S. A. L. de Andrade "Paramertical analysis of extended endplate semi-rigid joints subjected to bending moment and axial force," *Latin American Journal of Solids and Structures*,, pp. 39-59, 2007.
- [9]. Concepcion Diaz, Pascual Marti, Mariano Victoria, Osvalde M. Querin "Review on the modelling of joint behaviour in steel frames," *Journal of constructional steel research*, no. 67, pp. 741-758, 2011
- [10]. Ana Margarida Girao Coelho, CHARACTERIZATION OF THE DUCTILITY OF BOLTED END PLATE BEAM-TO-COLUMN STEEL CONNECTIONS, Coimbra: Universidade de Coimbra, 2004.